

Gamma-ray emission from massive stars interacting with AGN jets

Anabella T. Araudo¹, Valentí Bosch-Ramon² & Gustavo E. Romero^{3,4}

(1) Centro de Radioastronomía y Astrofísica - UNAM (2) Departament d'Astronomia i Meteorologia, Universitat de Barcelona (3) Instituto Argentino de Radioastronomía - CONICET (4) Facultad de Ciencias Astronómicas y Geofísicas - UNLP

Introduction

Active galactic nuclei (AGNs) consist of a supermassive black hole (SMBH) surrounded by an accretion disc in the center of a galaxy. Sometimes these objects present radio emitting jets originated close to the SMBH. Such jets are very weak or absent in radio-quiet AGNs, but in radio-loud sources bipolar powerful jets of collimated plasma are ejected perpendicular to the accretion disc. Radio-loud AGNs present (thermal and non-thermal) continuum emission in the whole electromagnetic spectrum, from radio to γ -rays.

In the nuclear region of AGNs there is matter in the form of diffuse gas, (BLR) clouds, and stars, making jet medium interactions likely (e.g. Araudo et al. 2010). We study the interaction of massive stars with the AGN jets (e.g. Komissarov 1994, Bednarek & Protheroe 1997, Barkov et al. 2010, Araudo et al. 2012, Huarte-Espinosa, M. et al. 2013). We analyze the dependence with the interaction height z of the double bow shock formed around each star interacting with the jets, and also the subsequent non-thermal processes generated at these shocks.

Jet-star interaction

We consider that massive stars ($m > 8M_{\odot}$) with mass loss rate and terminal wind velocity $\dot{M}_w = 10^{-6} M_{\odot} \text{ yr}^{-1}$ and $v_{\infty} = 2000 \text{ km s}^{-1}$, respectively, are surrounding the SMBH. The number density of these stars follow a power-law mass distribution: $dN_*/dV = Km^{-5.3} dm$, where we have considered the Salpeter initial mass function and that the lifetime of stars in the main sequence is $\sim 10(m/M_{\odot})^{-3}$ Gyr. In addition to that, we fix the mass density of all stars as $\rho = \rho_{pc}(z/1\text{pc})^{-y}$, where y is a free parameter that we fix in 1 and 2, and ρ_{pc} is determined through the relation between the star formation and SMBH accretion rate (Satyapal et al. 2005). We consider $M_{bh} = 10^7, 10^8$, and $10^9 M_{\odot}$. The density of massive stars around the SMBH (n_*), and number N_{*j} of massive stars contained inside the jet (of radius $R_j \sim 0.1z$) are shown in Fig. 1.

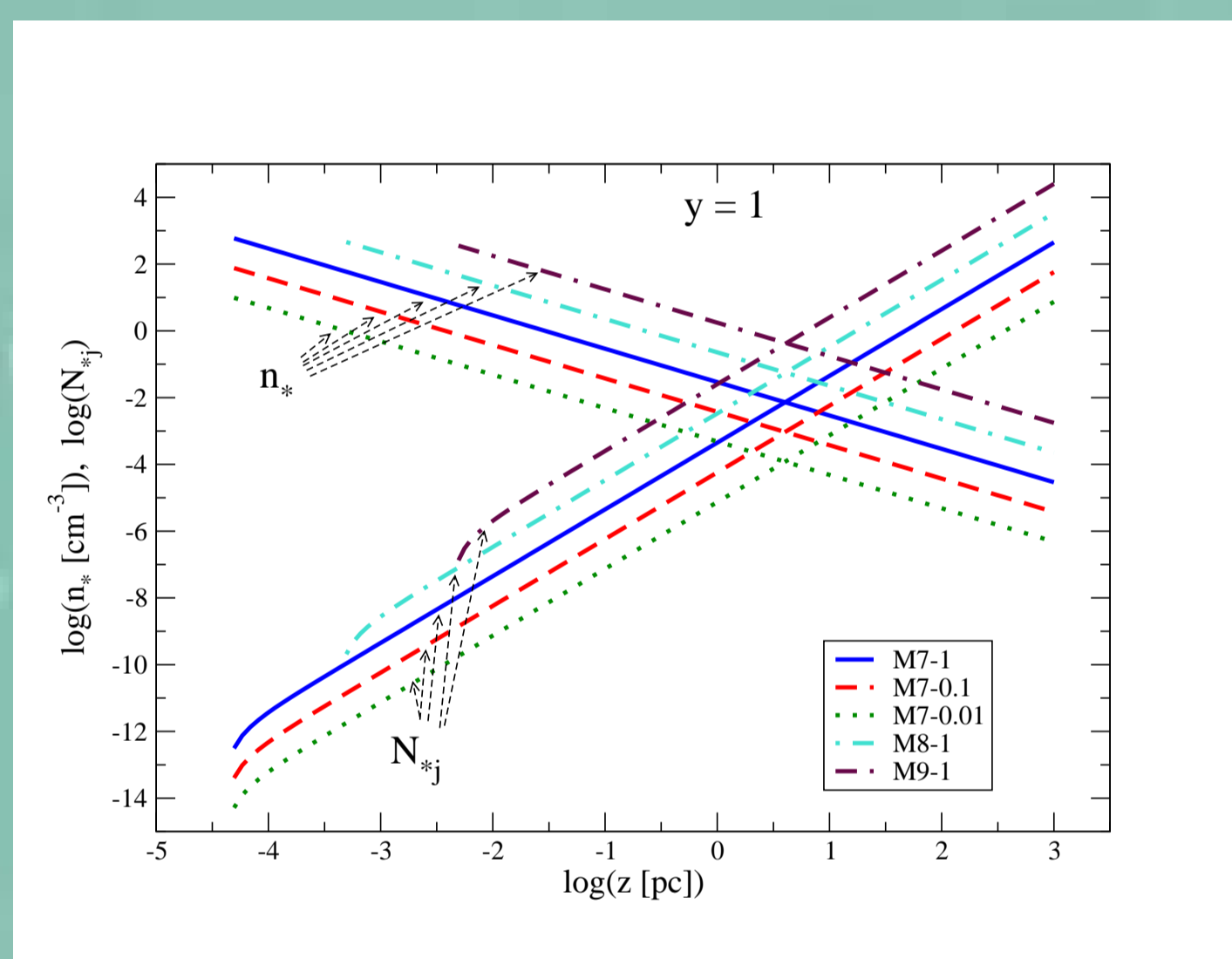


Figure 1: Density of massive stars (n_*) and number (N_*) of massive stars inside the jet for the different values of z . Cases for different combinations of M_{bh} and η_{acc} are plotted.

When the jet interacts with stars a double bow shock is formed around them, as is shown in Fig. 2. (In a first order of approximation, we neglect the details of the penetration of stars into the jet.) The location of the stagnation point is at a distance R_{sp} from the stellar surface, where the wind and jet ram pressures are equal. From $\rho_w v_{\infty}^2 = \rho_j c^2 \Gamma$, where $\rho_w \sim \dot{M}_*/(4\pi R_{sp,0}^2 v_w)$ is the wind density, we obtain

$$\frac{R_{sp,0}}{R_j} \sim 10^{-2} \left(\frac{\dot{M}_w}{10^{-6} M_{\odot}/\text{yr}} \right)^{1/2} \left(\frac{v_{\infty}}{2000 \text{ km/s}} \right)^{1/2} \left(\frac{L_{j0}}{10^{42} \text{ erg/s}} \right)^{-1/2}$$

We assume that the jet has a Lorentz factor $\Gamma = 10$ and a velocity $\sim c$. Note that $R_{sp,0} \propto z$.

The subscript 0 in $R_{sp,0}$ indicates that possible variations of the jet kinetic luminosity, L_j , with z produced by multiple jet/star interactions are neglected. However, the jet transfers a fraction $\sim (R_{sp}/R_j)^2$ of its kinetic energy to the bow shock that is formed around each star. With the aim of taking into account the decrease of L_{j0} by the interaction of many stars, we adopt an exponential dilution factor: $L_j(z) = L_{j0} \exp(-\tau)$, where $\tau = \int_{z_0}^z \pi R_{sp}^2 n_*(z') dz'$ takes into account the energy

loss per interaction multiplied by the number of stars within the jet up to z (i.e. the number of interactions). This provides the following solution:

$$R_{sp} \sim \frac{R_{sp,0}}{\sqrt{1 - \left(\frac{R_{sp,0}}{z}\right)^2 \pi \int_{z_0}^z n_*(z') z'^2 dz'}} = \frac{R_{sp,0}}{\sqrt{1 - \left(\frac{R_{sp,0}}{R_j}\right)^2 N_{*j}}}$$

where we have neglected that the jet can be reestablished after each interaction. L_{j0} is determined as $\eta_j L_{Edd}$, given $L_{j0} = 1.2 \times 10^{42} \eta_j (M_{bh}/10^7 M_{\odot})$, for $\eta_j = 0.1, 0.01$, and 10^{-3} .

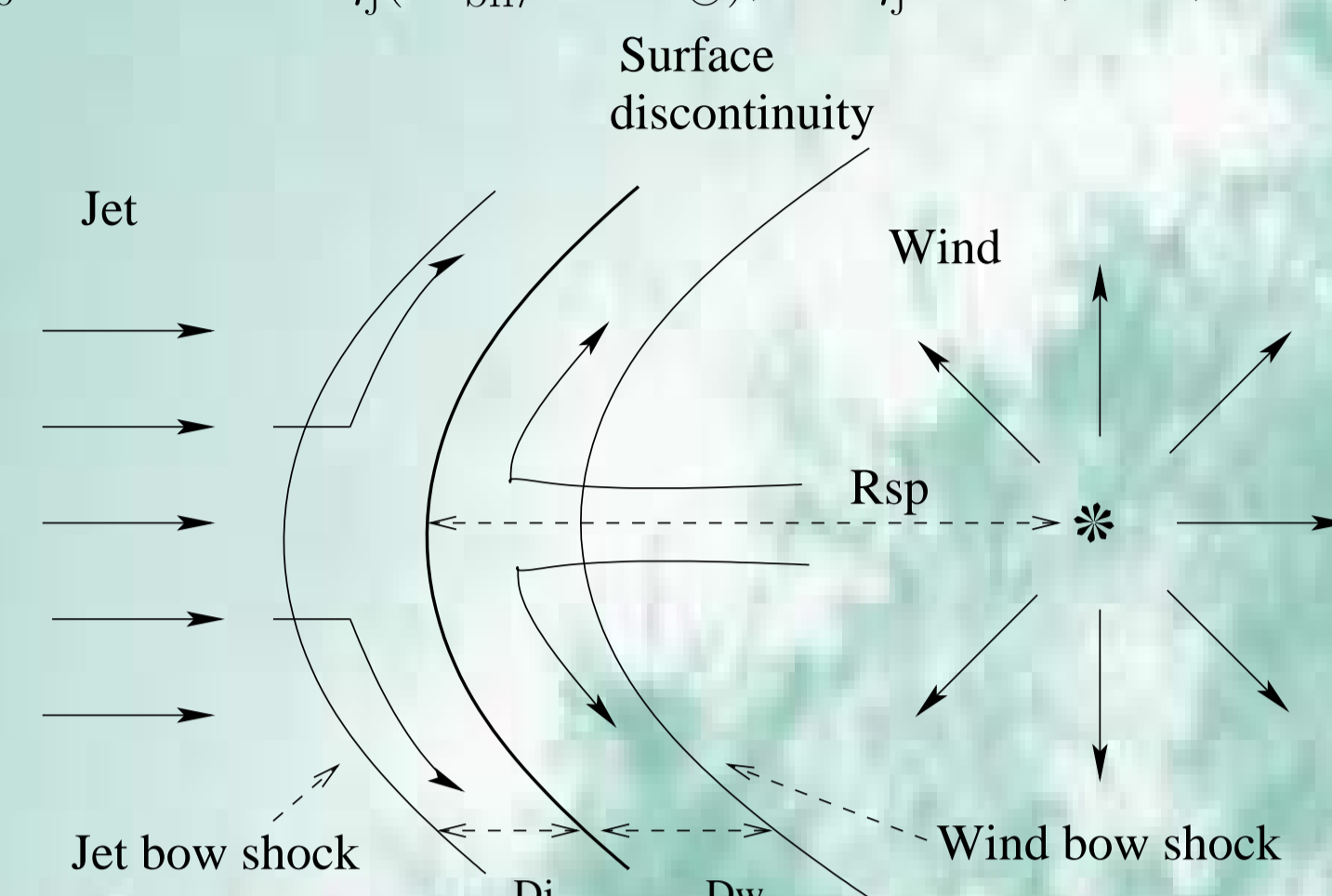


Figure 2: Sketch of the scenario. The size of the jet and wind shocked regions, D_j and D_w , respectively, are determined considering the conservation of the number particle density, obtaining $D_j \sim D_w \sim 0.3R_{sp}$.

Particle acceleration

Particles can be accelerated up to relativistic energies in both the jet and wind shocks. Relativistic electrons and protons are injected in the downstream regions following a distribution $Q_{e,p} \propto E_{e,p}^{-2}$. The luminosity of particles accelerated in the jet and in the wind bow shocks is $L_{ntj} \sim 0.1(R_{sp}/R_j)^2 L_j$ and $L_{ntw} \sim 0.1L_w/4$, respectively, where $L_w = \dot{M}_w v_{\infty}^2/2$.

We estimate the magnetic field in the jet shocked region, B_{jbs} , assuming that the magnetic energy density is a fraction η_B of the energy density of the jet shocked matter, resulting

$$B_{jbs} \sim 8.7 \times 10^{-3} \left(\frac{\eta_B}{0.01} \right)^{1/2} \left(\frac{L_j}{10^{42} \text{ erg s}^{-1}} \right)^{1/2} \left(\frac{z}{\text{pc}} \right)^{-1} \text{ G}$$

The main radiative losses that affect the evolution of Q_e are synchrotron radiation and external Compton (EC) scattering. For the later we have considered stellar target photons with an energy and luminosity $\sim 30 \text{ eV}$ and $L_* = 3 \times 10^{38} \text{ erg s}^{-1}$, respectively. In addition to radiative losses, electrons can escape from the emitter by advection or diffusion. The maximum energy achieved by electrons in the jet bow shock is determined by synchrotron losses at $z \lesssim z_E \equiv 0.17(\eta_B/0.001)^{-1/2}(L_j/10^{42} \text{ erg s}^{-1})^{1/2} \text{ pc}$, and by advection losses farther up:

$$E_e^{\text{max}} \sim \begin{cases} 1.2 \times 10^2 \left(\frac{\eta_B}{0.001} \right)^{-1/4} \left(\frac{z}{1\text{pc}} \right)^{1/2} \left(\frac{L_j}{10^{42} \text{ erg s}^{-1}} \right)^{-1/4} \text{ TeV} & z < z_E \\ 48.3 \left(\frac{\eta_B}{0.001} \right)^{-1/2} \text{ TeV} & z > z_E \end{cases}$$

For the wind we assume the Usov & Melrose (1992) parametrization of the magnetic field B_w , with a value in the stellar surface of about 10 G. Maximum energies for electrons accelerated in the wind bow shock are determined by IC scattering and diffusion (see Fig. 3).

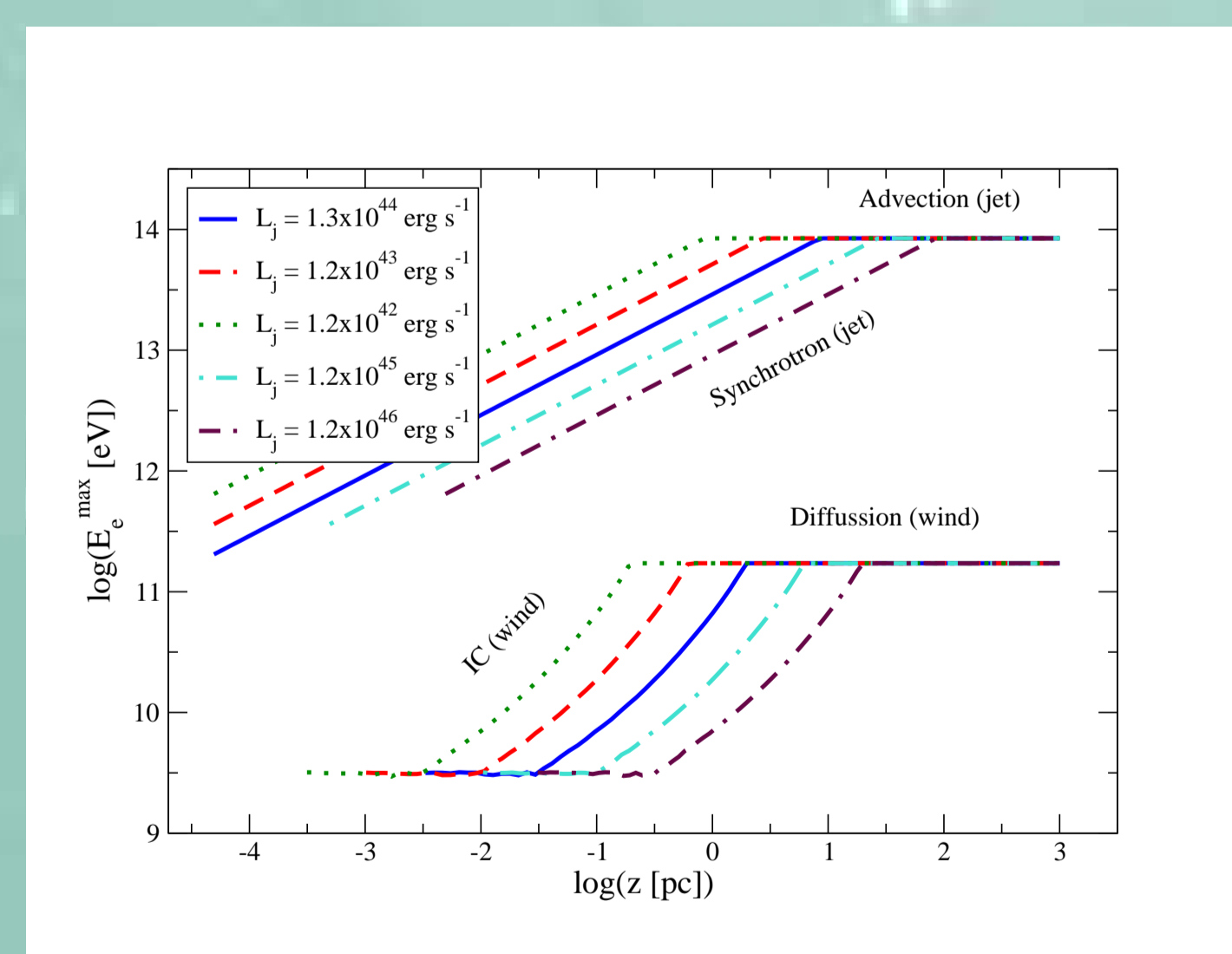


Figure 3: Maximum energies of electrons accelerated in the jet and wind bow shocks for different values of L_j .

Gamma-ray emission

The emission produced by massive stars per interaction at small values of z is higher than emission produced at larger z , as a consequence of the dilution of the target fields (the photon and matter densities decrease as z^{-2} and B_{jbs} as z^{-1}). However, at large values of z the number of stars interacting with the jet is > 1 and the emission produced by all of them increase as z . We calculate the emission produced by each one of the massive stars located inside the jet at each z and then we integrate along z all the contributions. Synchrotron emission produced in the jet bow-shock is about 100 times larger than the emission produced in the wind, but IC radiation generated in the jet and in the wind both reach the similar luminosity along z . In the jet region where $N_{*j} > 1$, R_{sp} is large enough to suppress the effect of photon-photon absorption.

In Fig. 4 we plot the bolometric luminosities achieved by different stellar populations with jets of different L_j . In the cases with low values of N_{*j} , the produced HE emission can not be detected by *Fermi* satellite (in the range 0.1-1 GeV) in any case. The most interesting case is that with $\eta_{acc} = 1$, which emission could be marginally detectable in the case of sources with $L_j \gtrsim 10^{44} \text{ erg s}^{-1}$ located at a distance $\lesssim 10 \text{ Mpc}$, similar to the distance ($\sim 4 \text{ Mpc}$) of the radiogalaxy Centaurus A. We note that the emission produced by jet/star interactions will be more prominent in AGNs with dense stellar populations. In particular, the interaction of a star forming region with a jet will be study by us in a future work.

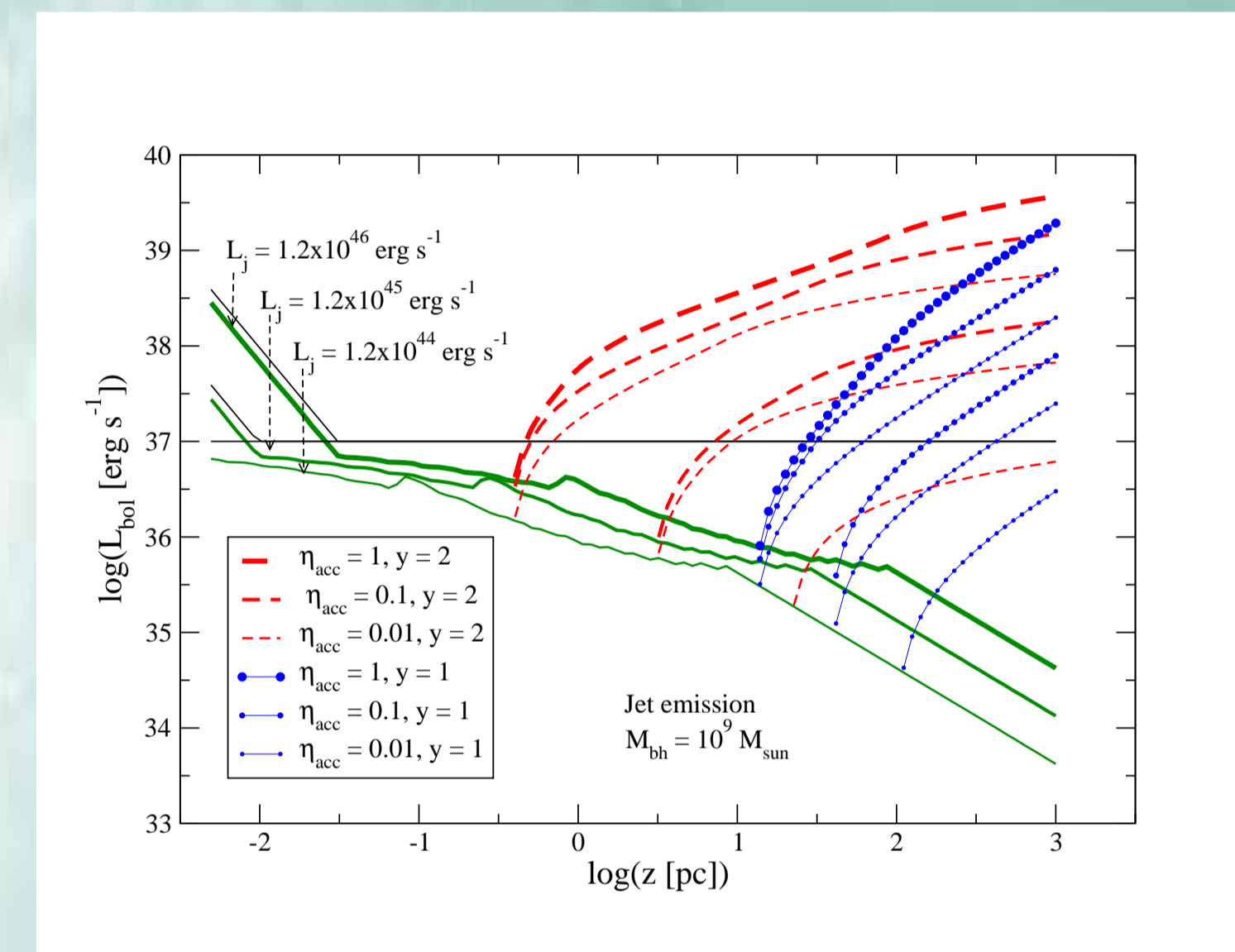


Figure 4: Bolometric luminosities produced by synchrotron, and IC along the jet.

Discussion

Since jet-star emission should be rather isotropic, it would be masked by jet beamed emission in blazar sources. Although radio loud AGN jets do not display significant beaming, these objects may emit γ -rays from jet-star interactions. The emission produced by many stars interacting with the jet will be rather steady. Misaligned radio loud AGNs represent an increasing population of GeV sources, as is shown in the second catalog of the *Fermi* γ -ray satellite. Close and powerful sources could be detectable by deep enough observations of *Fermi*. After few-year exposure times, a significant signal from these objects could be found, and their detection can shed light on the jet matter composition as well as on the stellar populations in the vicinity of AGNs.

References

- Araudo A., Bosch-Ramon V., Romero G. 2010, A&A 522, 97
Araudo A., Bosch-Ramon V., Romero G. 2012, AIPC 1505, 614
Barkov M., Aharonian F., Bosch-Ramon V. 2010, ApJ 723, 1517
Bednarek W. & Protheroe R. 1997, MNRAS 287, L9
Huarte-Espinosa M. et al. 2013 [arXiv-1301.7081] Komissarov S. 1994, MNRAS 269, 394
Satyapal S. et al. 2005, ApJ 633, 86

Contact person: Anabella Araudo (a.arauado@crya.unam.mx)